Interface effects on the critical temperature of heterostructures of magnetic films

J T Ou†§, W Lai†, D L Lin† and Felix Lee‡

† Department of Physics, State University of New York, Buffalo, NY 14260-1500, USA
‡ Department of Physics, National Tsing Hua University, Hsinchu, Taiwan, Republic of China

Abstract. The analytical approach to the critical point of Ising films proposed recently by Lin *et al* is extended to investigate the interface effects on the critical temperature T_c for magnetic bilayer heterostructures. We consider heterostructures composed of an m-monolayer film grown on a substrate of an n-monolayer magnetic film with different lattice structures where $1 \leqslant m$ and $n \leqslant \infty$. The mean $T_c(m, n)$ of the bilayered heterostructure as a whole is obtained as a function of the total thickness $N = m + n$ of the inhomogeneous system. A strong dependence of the critical temperature upon the lattice structure is revealed. In particular, interface effects on T_c for systems consisting of an overlayer of a few spin monolayers on a thin film of magnetic substrates with different lattice structure are investigated in detail and results for various combinations of the lattice structure are discussed.

1. Introduction

The technology of molecular epitaxy has made it possible to study properties of materials in reduced dimensionality that do not usually exist in the three-dimensional (3D) solids. A great deal of work has been carried out on various kinds of crystalline solid in the form of thin films, heterostructures and superlattices. In particular, a number of experiments on the critical behaviour of magnetic thin films can be found in the literature of recent years [1–9].

Numerical calculation of the critical temperature T_c for a film of seven spin monolayers was performed with the high-temperature-series-expansion-extrapolation (HTSEE) method up to twelfth order [10]. More recently, an analytical method has been developed on the basis of the variational cumulant expansion (VCE) to calculate the critical point of Ising films to an arbitrary accuracy [11]. For the first time $T_c(l)$ was calculated analytically as a function of the film thickness where l is the number of spin monolayers in the film. The theory is based on the conjecture that T_c is determined by locating the bifurcation point of the free energy, which is regarded as an analytic function of the temperature when the variational parameter introduced into the VCE is set to yield the minimum free energy for the system. From the recursion formula for cumulants, it can be shown that T_c is given by the ratio of the second-order derivative of two successive cumulants to any order of accuracy. As the cumulants are calculated analytically by a graph technique, we can derive an analytical expression for T_c. In this way, the critical temperature is obtained to the fourth order for simple cubic (sc) and body-centred cubic (bcc) and to the third-order for face-centred cubic (fcc) lattices [11, 12]. It is found that the strong dependence of T_c on

§ On leave of absence from Nankai University, Tianjin 300071, People's Republic of China.

the lattice structure is solely determined by the number of nearest neighbours (ns) of the lattice point. T_c increases quickly with increasing coordination number. On the other hand, the dimensionality cross-over region is rather narrow in all three cases. The film behaves like a two-dimensional (2D) system for $l < 3$ and like a 3D bulk for $l > 6$.

When compared with experimental data measured for ultrathin Ni films along both the crystal growing directions (001) and (111) [13], the predicted critical temperature appears to increase too rapidly with l for $l < 4$. It has been shown, however, that excellent agreement with experiments can be achieved by introducing variable exchange integrals near the surfaces [14].

As it is likely that heterostructures consisting of magnetic films of various lattice structures with well defined interfaces may be available for experiments, it should be very interesting to investigate the interface effects on the critical temperature in such materials. We extend, in this article, the method developed in [11] and [12] to treat the critical point of magnetic bilayer heterostructures. Our purpose is to study the behaviour of the critical temperature $T_c(m, n)$ for a system consisting of m spin monolayers over a magnetic substrate of n monolayers with different lattice structure as a function of n and m, both of which can take any integer value.

The VCE theory for the critical point is reviewed in section 2, in which the difficulty of higher-order calculations in the usual treatment is discussed. In section 3, we outline very briefly the method of calculation with the emphasis on the procedures of graph counting for various heterostructures. The results for various combinations of lattices are presented and discussed in section 4.

2. Theory

An Ising spin system in the absence of an external field is characterized by the Hamiltonian

$$H = -\frac{1}{s^2} \sum_{\langle i,j \rangle} J_{ij} s_i^z s_j^z. \tag{1}$$

Throughout this article, we follow the same notation as that in [11] and [12] unless otherwise specified. In terms of the dimensionless quantities $\beta_{ij} = j_{ij}/k_B T$ and $t_i = s_i^z/s$, the action S for the system is given by

$$S = \frac{X}{k_B T} = -\sum_{\langle i,j \rangle} \beta_{ij} t_i t_j \tag{2a}$$

with the corresponding trial action for the noninteracting system

$$S_0 = \sum_i \xi_i t_i. \tag{2b}$$

Here, $X = k_B T S$ and we have introduced the variational parameters ξ_i which serve as the order parameters for our system as has been pointed out in [11].

The partition function of the system is

$$Z = e^{-W} = \sum e^S = \sum e^{S-S_0} e^{S_0} = Z_0 \langle e^{S-S_0} \rangle_0 \tag{3a}$$

where we have defined the free energy W, and the Boltzmann ensemble average

$$\langle \ldots \rangle_0 = \frac{1}{Z_0} \sum_{t_i} (\ldots) \exp(\xi_i, t_i). \tag{3b}$$

The partition function for a corresponding noninteracting system with free energy W_0 is

$$Z_0 = e^{-W_0}. \tag{3c}$$

Thus the free energy is given by

$$W = W_0 - \ln \langle e^{S-S_0} \rangle_0 = W_0 - \ln \left[1 + \sum_{n=1}^{\infty} \frac{1}{n!} \langle (S - S_0)^n \rangle_0 \right]$$

$$= W_0 + \sum_{v=1}^{\infty} \frac{(-1)^v}{v} \left[\sum_{n=1}^{\infty} \frac{1}{n!} \langle (S - S_0)^n \rangle_0 \right]^v \tag{4}$$

after the expansion of the exponential and logarithmic functions. In terms of the VCE, (4) takes a much simpler form. Up to the order m, we have

$$W \approx W_0 - \sum_{n=1}^{m} \frac{1}{n!} \langle (S - S_0)^n \rangle_c = W_{eff,m} \tag{5}$$

where the cumulant average over the Boltzmann weight e^{S_0} is defined by $\langle \ldots \rangle_c$. The relation between the two averages of a quantity can most easily be established by a comparison of the corresponding terms in expansions of (4) and (5).

For simplicity, we consider a uniform spin-$\frac{1}{2}$ film with $\beta_{ij} = \beta$ and $\xi_i = \xi$. The formalism is, however, completely general and applies to Ising systems with different spin values and spatially dependent quantities β_{ij}. The first-order free energy is then

$$(1/N)W_{eff,1} = -\ln(2\cosh \xi) - (d/\Theta)y^2 + \xi y \tag{6a}$$

$$y = \tanh \xi \tag{6b}$$

where d represents the dimensionality and $\Theta = k_B T/J = 1/\beta$ is the reduced temperature. By minimizing the free energy, we find the condition

$$\tanh \xi = (\Theta/2d)\xi \tag{7}$$

which determines the variational parameter.

As has been discussed in [11], (7) has different solutions in different temperature ranges for a given dimensionality d, and the analytic behaviour of these solutions is illustrated in figure 1. When $\Theta \geqslant \Theta_c$, there is only one solution $\xi_0 = 0$ corresponding to the minimum of $W_{eff,1}$. When $\Theta < \Theta_c$, there are three solutions ξ_0 and $\xi_\pm$ corresponding to the maximum and minima of the function $\dot{W}_{eff,1,}$, respectively. Thus, the critical value Θ_c is determined by the bifurcation point of $W_{eff,1}(\Theta, \xi)$ for $\xi = 0$. The parameter ξ is zero in the high-temperature region and becomes nonzero in the low-temperature region. Hence it has the properties of the order parameter in Landau theory. On the basis of this analysis, a conjecture was proposed [11] that, to any order of the VCE, the critical temperature is determined by locating the bifurcation point of the free energy $W_{eff,m,}$, namely, by the condition

$$(\partial^2/\partial \xi^2)W_{eff,m}(\Theta_c, \xi)|_{\xi=0} = 0. \tag{8}$$

An important remark is in order at this point. Without this conjecture one can only be sure that, in the first-order approximation, $\xi = 0$ corresponds to a minimum of the function $W_{eff,1}(\Theta, \xi)$ for $\Theta \geqslant \Theta_c^{(1)}$. This presents a difficulty in higher-order calculations of the internal energy and leads to the so-called 'unwanted first-order phase transition' [15, 16]. With the conjecture (8), it can be shown that $W_{eff,m}(\Theta, 0)$ remains analytic for $\Theta < \Theta_c^{(m)}$ which is always lower than $\Theta_c^{(1)}$. The extremum condition like (7) for the first order can be solved for every order. In fact we have approximately solved these equations up to $m = 8$ for Θ not far below $\Theta_c^{(m)}$ [17]. Once Θ becomes less than $\Theta_c^{(m)}$, the minimum free energy is characterized by $\xi_\pm^{(m)}$. As long as the variational parameter is so chosen that the free energy remains a minimum continuously across the critical point, there will not be any discontinuity in the internal energy, and hence no first-order phase transition will appear.
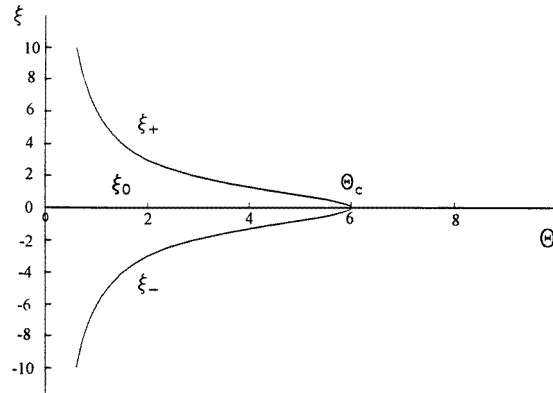
Figure 1. The analytic behaviour of the solutions to (7). The critical point is determined by the bifurcation point Θ_c.

3. Method of calculation

As has been shown in [11], one can prove by mathematical induction that (8) reduces to

$$[(\partial^2/\partial\xi^2)\langle S^{m-1}\rangle_c - (1/m)(\partial^2/\partial\xi^2)\langle S^m\rangle_c]_{\xi=0} = 0 \qquad m \geqslant 2 \tag{9}$$

which yields immediately the critical temperature

$$k_B T_c^{(m)} = (1/m)[(\partial^2/\partial\xi^2)\langle X^m\rangle_c/(\partial^2/\partial\xi^2)\langle X^{m+1}\rangle_c]_{\xi=0} \qquad m \geqslant 2. \tag{10}$$

Note that $X = k_B T S$ as defined in (2a) and the energy is in the unit of J. The cumulants $\langle S^m\rangle_c$ are calculated from the first-order moment

$$\langle S\rangle_0 = \tfrac{1}{2}\sum_{i,j}\beta_{ij}y_iy_j = \langle S\rangle_c \tag{11}$$

with the help of the recursion formula for moments

$$\langle S^{p+1}\rangle_0 = \left(\tfrac{1}{2}\sum_{\langle i,j\rangle}\beta_{ij}\frac{\partial^2}{\partial\xi_i\partial\xi_j} + \sum_{\langle i,j\rangle}\beta_{ij}y_i\frac{\partial}{\partial\xi_j} + \langle S\rangle_c\right)\langle S^p\rangle_0 \tag{12}$$

and relations between $\langle S^p\rangle_c$ and $\langle S^p\rangle_0$ where β_{ij} measures J_{ij} in the unit of $k_B T$ and p is an integer.

The procedure is standard but quickly becomes complicated as m increases. The amount of work is, however, greatly reduced by a graph technique described in detail in [12]. It is equivalent to the random walk calculation and the major part of the work involves the counting of topologically equivalent graphs to be summed. For simplicity, we still assume in what follows a uniform coupling β throughout the heterostructure of different lattices, although the method is completely general and applies to inhomogeneous lattices of various geometry. Thus, (20)–(22) of [12] expressing T_c in terms of the number of various graphs remain valid.

We consider only cubic lattices in the present study. A heterostructure consists of a magnetic substrate of n monolayers, on top of which a magnetic film of m monolayers of different lattice is built. Thus the total number of spin monolayers in the structure is $N = n + m$. It is important to note that either m or n can take any positive integer value, and hence the bilayer system may be regarded as a 2D film with very few monolayers or may actually be a 3D bulk structure depending on the thickness N. It is also noted that
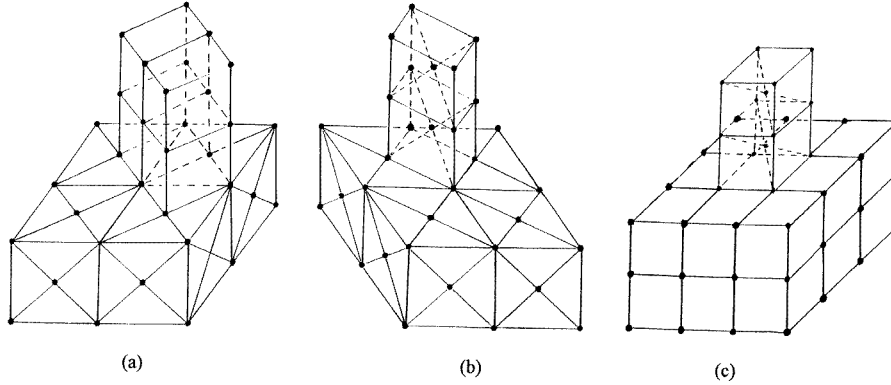
Figure 2. A schematic illustration of bilayer heterostructures composed of (a) sc–fcc, (b) bcc–fcc and (c) bcc–sc lattices.

every monolayer in the structure must contain exactly the same number of spins. For the purpose of the counting of monolayers only, the top surface of the substrate is regarded as the interface of the structure. Figure 2 illustrates the three cases for which T_c is calculated.

The number of graphs in which two nearest-neighbouring sites are connected by a bond is represented by $[l, l + \mu]$, and these connected graphs are embedded on the site l. Thus, $[l, l + \mu] = 6$ for bulk sc, 8 for bulk bcc and 12 for bulk fcc lattices. However, this number changes for sites on either of the surfaces and on the interface of a heterostructure. On the surface, $[l, l + \mu]$ becomes 5 for sc, 4 for bcc and 8 for fcc lattices. For sites on the interface, we have $[l, l + \mu] = 9$ for the sc–bcc structure. On the other hand, $[l, l + \mu] = 9$ for lattice sites on the sc–fcc interface and 12 for sites on the bcc–fcc interface.

For graphs that involve two bonds, the number of connected graphs for sites on the interface, and the surfaces as well as their immediate neighbouring monolayers are all different and have to be counted separately. As graphs involving more and more bonds must be counted in higher-order calculations, the procedure becomes tedious but remains straightforward. According to the prescription outlined above, we find the number of topologically equivalent graphs of different types needed for the three heterostructures of $(m + n)$ monolayers as follows. For sc–bcc structures, we have up to fourth-order

$$[l] = m + n \qquad\qquad\qquad m \geqslant 1, n \geqslant 2$$
$$[l, l + \mu] = 6m + 8n - 4 \qquad\qquad m \geqslant 1, n \geqslant 2$$
$$[l, l + \mu, l + \nu] = 36m + 64n - 42 \qquad\qquad m \geqslant 1, n \geqslant 2$$
$$[l, l + \mu, l + \nu, l + \eta] = 216m + 512n - 322 \qquad\qquad m \geqslant 1, n \geqslant 2$$
$$[l, l + \mu + \nu, l + \eta] = 216m + 512n - 400 \qquad\qquad m \geqslant 2, n \geqslant 3$$
$$[l, l + \mu + \nu + \eta, l + \delta] = 1296m + 4096n - 3422 \qquad\qquad m \geqslant 3, n \geqslant 4$$
$$[l, l + \mu + \nu + \eta = l + \delta] = 90m + 216n - 216 \qquad\qquad m \geqslant 2, n \geqslant 3. \qquad (13)$$

For sc–fcc structures, we have up to third-order

$$[l] = m + n \qquad\qquad\qquad m \geqslant 1, n \geqslant 2$$
$$[l, l + \mu] = 6m + 12n - 8 \qquad\qquad m \geqslant 1, n \geqslant 2$$
$$[l, l + \mu, l + \nu] = 36m + 144n - 154 \qquad\qquad m \geqslant 1, n \geqslant 2$$
$$[l, l + \mu + \nu, l + \eta] = 216m + 1728n - 2416 \qquad\qquad m \geqslant 3, n \geqslant 4$$
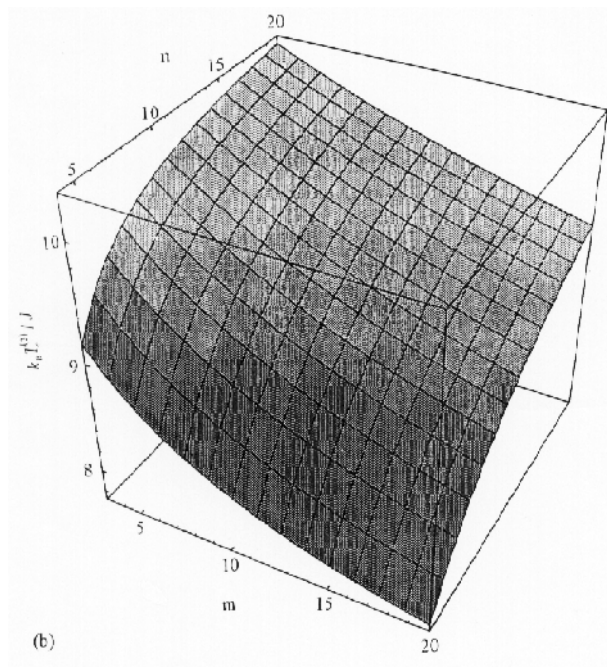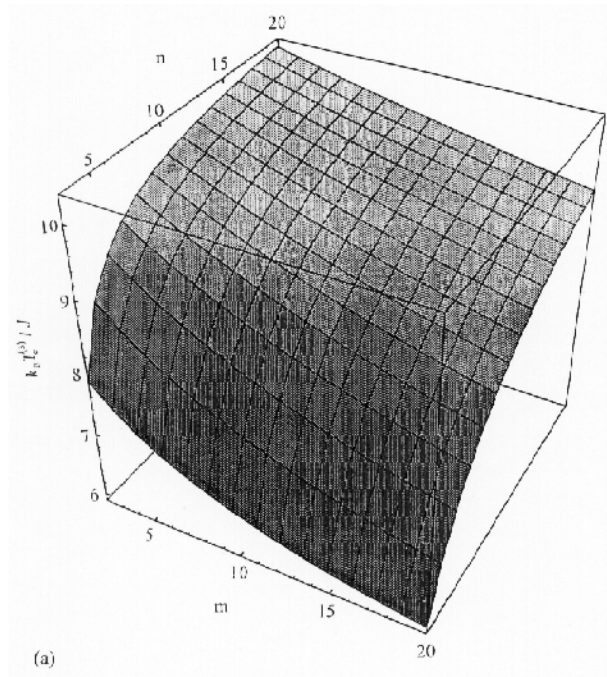$$[l, l + \mu + \nu = l + \eta] = 48n - 48 \qquad\qquad\qquad n \geqslant 2 \qquad (14)$$

Figure 3. The reduced critical temperature plotted as a function of the monolayer numbers m and n for heterostructures with an n-monolayer substrate and m monolayers added on its top surface: (a) $k_B T_c^{(3)}/J$ for sc–fcc; (b) $k_B T_c^{(3)}/J$ for bcc–fcc; (c) $k_B T_c^{(4)}/J$ for sc–bcc.
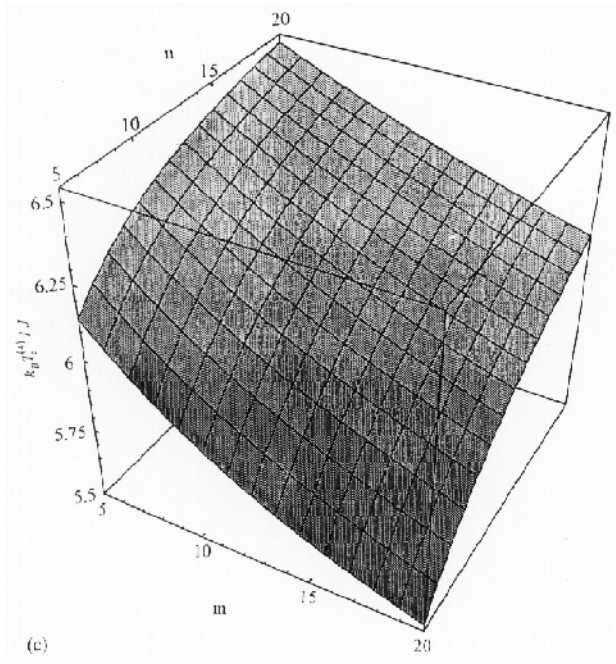
Figure 3. (Continued)

and for bcc–fcc structures, we find to third order

$$[l] = m + n \qquad\qquad m \geqslant 1, n \geqslant 2$$
$$[l, l + \mu] = 8m + 12n - 8 \qquad\qquad m \geqslant 1, n \geqslant 2$$
$$[l, l + \mu, l + \nu] = 64m + 144n - 128 \qquad\qquad m \geqslant 1, n \geqslant 2$$
$$[l, l + \mu + \nu, l + \eta] = 512m + 1728n - 1856 \qquad\qquad m \geqslant 3, n \geqslant 4$$
$$[l, l + \mu + \nu = l + \eta] = 48n - 48 \qquad\qquad n \geqslant 2. \qquad (15)$$

4. Results and discussion

The graph counting is carried out up to the fourth order for sc and bcc lattices, but only to the third order for structures involving the fcc lattice. This is because the bonds may form closed loops in each of these cases. As has been pointed out in [12], the term corresponding to a closed loop represents the contribution from the self-correlation of the initial spin at l, and is expected to be much more important than other graphs of the same order. In other words, the fourth-order correction improves the resulting T_c more significantly than the third-order correction in cases of sc and bcc lattices, while it is relatively small as compared to the third-order correction in the case of the fcc lattice.

In order to distinguish the lattice structure, we always assume in our calculation of the critical temperature that the substrate has at least three monolayers or $n \geqslant 3$, and that the over-layer film has at least two monolayers, namely, $m \geqslant 2$. Thus, the critical temperature T_c for sc–fcc structures calculated to the third-order is given by

$$k_B T_c^{(3)}/J = (444m + 4200n - 6196)/(90m + 396n - 438) \qquad m \geqslant 2, n \geqslant 3. \qquad (16)$$
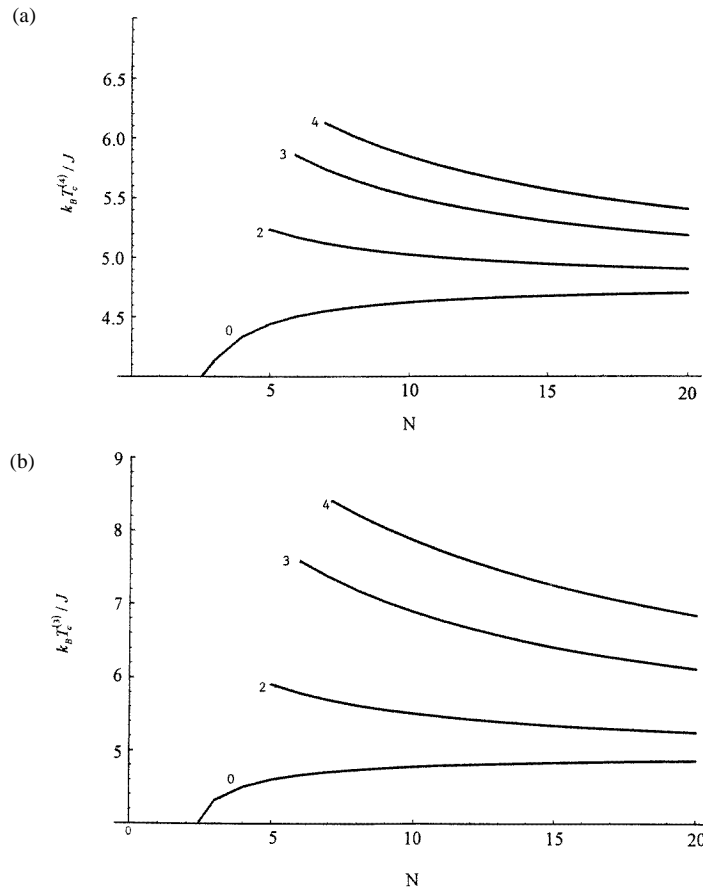
Figure 4. The reduced critical temperature versus the thickness of (a) bcc–sc and (b) fcc–sc heterostructures. The numeral besides a curve indicates the number of spin overlayers in the structure.

For bcc–fcc structures, the values of $k_B T_c^{(3)}/J$ are found for various cases and the results are shown in table 1. The results appear more complicated for sc–bcc structures because the fourth-order calculation involves more graphs. In table 2, we list $k_B T_c^{(4)}/J$ for various combinations of m and n in sc–bcc heterostructures.

In addition, we also present in figure 3 three-dimensional plots of $T_c(m, n)$ for the heterostructures illustrated in figure 2. For all three cases, it is seen that the critical temperature increases with increasing n (the number of monolayers in the substrate) for a fixed m (the number of monolayers of the overlayer film). On the other hand, it decreases with increasing m for a given n. This is because we are considering only cases in which the coordination number of the substrate is bigger than that of the overlayer film. As we have noted earlier, T_c is higher for materials of larger coordination number.

That T_c actually decreases when overlayers are added to a substrate with a larger coordination number may be demonstrated by a simple example. Consider a slab of fcc substrate whose T_c (expressed in $k_B T_c/J$) is around ten according to figure 5 of [12]. When overlayers of sc lattice are added on top of it, the transition temperature of the resulting
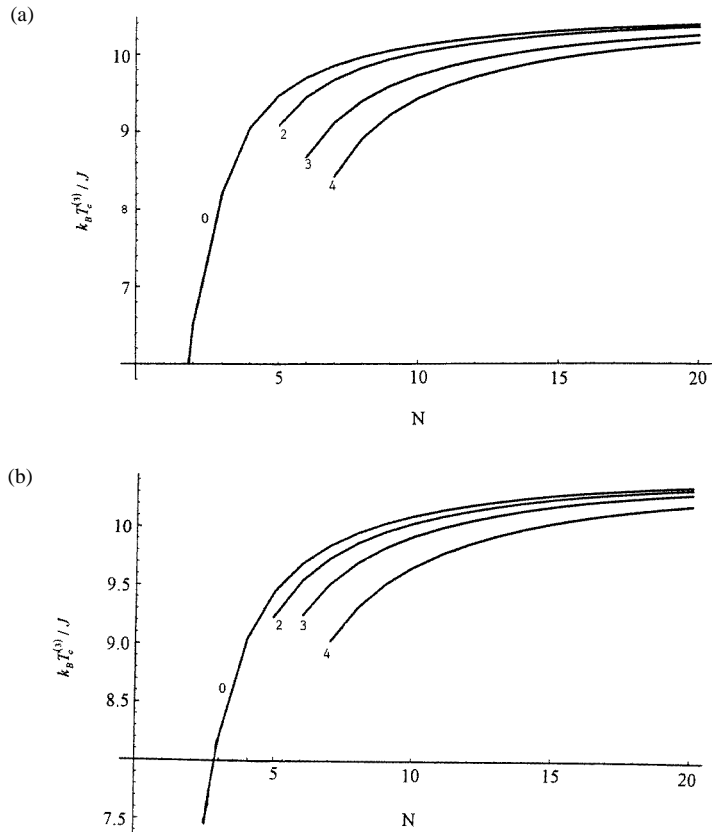
(a)

(b)

Figure 5. The same as in figure 4 except for (a) sc–fcc and (b) bcc–fcc heterostructures.

Table 1. The third-order critical temperature $k_B T_c^{(3)}/J$ calculated for various combinations of bcc–fcc structures.

n	$m \geqslant 3$	$m = 2$
$\geqslant 4$	$\dfrac{1168m + 4200n - 4672}{168m + 396n - 384}$	$\dfrac{4200n - 2336}{396n - 12}$
3	$\dfrac{1168m + 7928}{168m + 804}$	9.0035

structure is expected to decrease. This is most easily seen if the overlayer is much thicker than the substrate so that the structure is dominated by sc monolayers. The combined system then behaves more like an sc lattice with a T_c close to 4.5 according to figure 2 of [11]. This should not be taken as a contradiction to the well known fact that adding new bonds increases the critical temperature [18], which is always true in homogeneous spin systems without any interface effect involved.

To explore the interface influence on T_c for systems with an overlayer of just a few monolayers, we plot in figures 4–6 the critical temperature as a function of the thickness $N = m + n$ for various cases. We first consider heterostructures with sc substrates. The reduced critical temperature is shown in figure 4 for (a) bcc overlayers and (b) fcc overlayers.

Table 2. The fourth-order critical temperature $k_B T_c^{(4)}/J$ calculated for various combinations of sc–bcc structures.

n	$m \geqslant 5$	$m = 4$	$m = 3$	$m = 2$
$\geqslant 6$	$\dfrac{2118m + 7832n - 6782}{444m + 1168n - 956}$	$\dfrac{7832n + 1690}{1168n + 820}$	$\dfrac{7832n - 2588}{1168n - 56}$	
5	$\dfrac{2118m + 32378}{444m + 4884}$	6.1336	6.2310	6.2980
4	$\dfrac{2118m + 24546}{444m + 3716}$	6.0120	6.1212	6.2476
3	$\dfrac{2118m + 16330}{444m + 2548}$	5.7359	5.8464	5.9802

Table 3. The relative strength of the exchange integral in monolayers near film surfaces for Ni(111) and Ni(001).

	$m = 1$		$m = 2$		$m = 3$	
	a_1	b_1	a_2	b_2	a_3	b_3
fcc (111)	0.65	0.38	1.00	0.64	1.00	1.00
fcc (001)	0.17	0.14	0.66	0.45	1.00	0.76

Since both the bcc and fcc lattices have a larger coordination number than the substrate lattice, T_c for the heterostructure is higher than that of the substrate in both cases. It increases further as more monolayers are added. Because of the interface, in which every site has nine nns, the increase in T_c is enhanced and is particularly appreciable when the substrate is thin. As the substrate becomes thicker, the increase becomes smaller and eventually diminishes for large N as expected.

The critical temperature of heterostructures with fcc substrates is shown in figure 5 for (a) sc and (b) bcc overlayers. Since the substrate, in the present case, has a larger coordination number than either of the overlayer lattices, T_c for the heterostructure is in general lower than the substrate. The more overlayers added to the top, the lower a T_c results. The interface effect, however, is relatively insignificant as compared to the previous cases because the coordination number of the substrate is twelve in the present case. Again, the change in T_c vanishes in the limit of large N as it should.

The interface effect is most remarkable in sc–bcc heterostructures with bcc substrates. Figure 6 shows the critical temperature behaviour for such structures with (a) sc and (b) fcc overlayers. It is observed that for fcc–bcc, T_c changes in a similar fashion as those in figure 4 because the nn number for fcc is larger than that for bcc. In figure 6(a), however, one sees that up to three sc monolayers added to a bcc substrate result in a higher T_c than that of the bcc substrate film. Only when four or more monolayers are added does the resulting T_c for the heterostructure become lower than that of the substrate. This unusual phenomenon is actually due to the interface. We note that the number of ns for a site in the sc–bcc interface is nine, which is larger than that for either of the component bulk lattices. Hence our result simply indicates that more than three sc monolayers are needed to compensate the effect of the interface before the critical temperature of the heterostructure becomes lower than that of the substrate.

Finally, we emphasize that, in our treatment of magnetic systems of reduced dimensionality on the Ising model, the only factor that results in the difference from the bulk is the nn number which is different for sites on the surface, on the interface and in the bulk. For a sc magnetic film of finite thickness, our results converge quickly to the
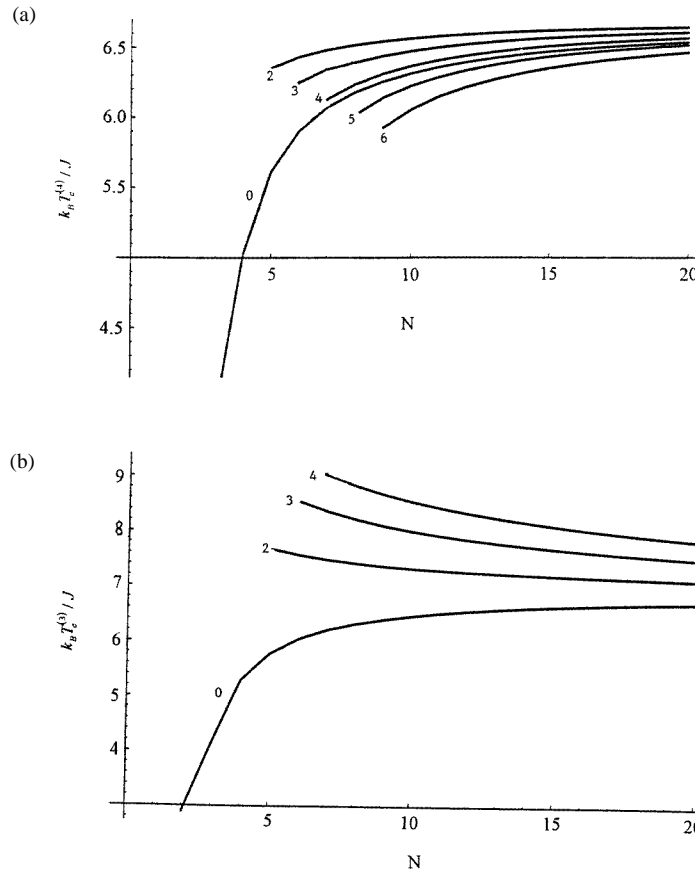
(a)

(b)

Figure 6. The same as in figure 4 except for (a) sc–bcc and (b) fcc–bcc heterostructures.

numerical results from the twelfth-order HTSEE [10]. As a matter of fact, the exchange coupling in a thin film may be very different from that in the bulk. It has been suggested [19] and confirmed [20] that the surface layer of a ferromagnet follows a spin wave $T^{3/2}$ law, but with a surface Bloch parameter $b_s = \alpha_s b_{bulk}$ enhanced by a factor $\alpha_s = 2$ if the exchange remains homogeneous up to the surface. It has also been shown later that a reduced exchange strength in the surface can cause a further enhancement, resulting in $\alpha_s > 2$ [21]. Such enhancement of the surface spin wave parameter has been observed in recent experiments [22, 23], indicating the reduced exchange coupling in the surface.

The present theory can easily be generalized to include the inhomogeneous coupling. For example, the surface coupling J_s may be different from the bulk J_b, and the intraplane $J_\parallel$ may be different from the interplane $J_\perp$. This will complicate the procedure of graph counting considerably, but will not introduce any essential difficulty. We have found in our second-order calculation that a slight anisotropy of the coupling strength J, say, $J_\perp = 0.9J_\parallel$, may reduce T_c appreciably [24]. The contribution from the next-nearest-neighbour (nnn) coupling to the critical behaviour has also been explored in [24]. Second-order results indicate that T_c increases significantly even if one assumes that the nnn coupling is one order of magnitude weaker than the nn coupling.
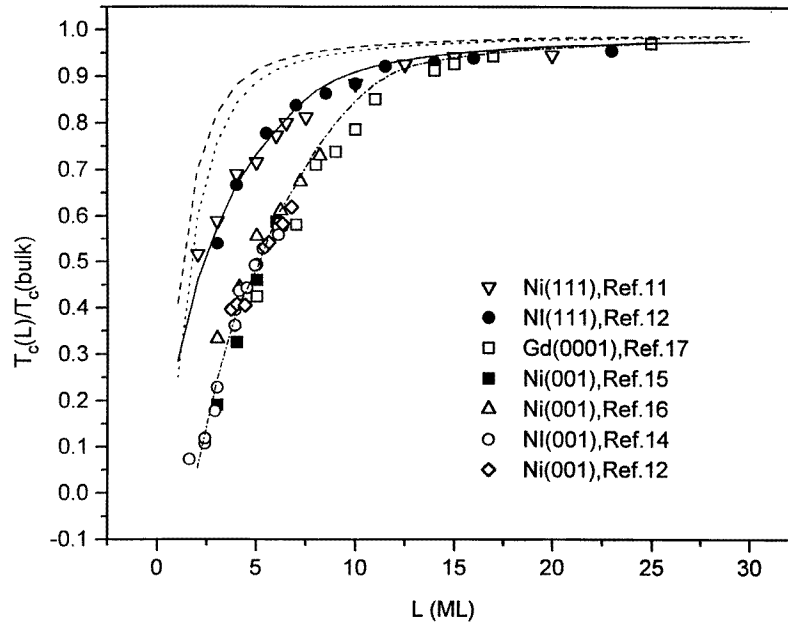
Figure 7. A comparison between the theory and experiments: the critical temperature as a function of the film thickness calculated with constant and variable coupling for fcc films is compared with the data measured on ultrathin Ni films. The theoretical T_c for a constant-coupling film with (111) and (001) surfaces is given by the dashed and dotted lines, respectively. The solid and dash–dotted lines correspond to results for fcc (111) and (001) films with variable exchange coupling specified in table 3.

To our knowledge, there is no experimental data in the literature for the critical temperature of magnetic heterostructures. There does exist, however, a series of systematic measurements of T_c as a function of thickness for ultrathin fcc Ni films in both (111) and (001) directions [13]. Since the cubic symmetry is broken near the film surface, resulting in uniaxial anisotropy, hence the system may be treated by the Ising model. Following the procedure described in [12], we find that the data can be reproduced very well by allowing variable coupling in only a couple of monolayers near the surfaces. We assume that $J_\parallel = \alpha_i J$ and $J_\perp = b_i J$, where i labels the monolayer with $i = 1$ at the surface. It is assumed further that the parameters $a_i < a_{i+1} < 1$ and $a_i > b_i$. The results are compared with data in figure 7 and the parameters that fit the data best are listed in table 3. It turns out that the reduction of the surface coupling we find here is consistent with recent measurements of the enhancement of the spin wave parameter [22, 23].

It may be of interest to mention that the method we have developed can also be applied to calculate analytically the mean magnetization of magnetic films and heterostructures. Work along this direction is being carried out and results will be reported elsewhere.

Acknowledgments

References

[1] See, for example, Falicov L M, Mejia-Lira F and Moran-Lopez Y L (eds) 1990 *Magnetic Properties of Low-Dimensional Systems II (Springer Proceedings in Physics 50)* (Berlin: Springer)
[2] Stampanoni M, VaterlausA, Aeschlimann M and Meier F 1987 *Phys. Rev. Lett.* **59** 2483
[3] Dürr W, Taborelli M, Paul O, Germar R, Gudat W, Pescia D and Landolt M 1989 *Phys. Rev. Lett.* **62** 206
[4] Liu Z C and Bader S D 1990 *J. Appl. Phys.* **67** 5758
[5] Schneider C M, Bressler P, Schuster P and Kirschner J 1990 *Phys. Rev. Lett.* **64** 1059
[6] Ballentine C A, Fink R L, Araya-Pochet J and Erskine J L 1990 *Phys. Rev.* B **41** 2631
[7] Li Y, Farle M and Baberschke K 1990 *Phys. Rev.* B **41** 9596
[8] Qiu Q, Pearson J and Bader S D 1991 *Phys. Rev. Lett.* **67** 1646
[9] Li Y and Baberschke K 1992 *Phys. Rev. Lett.* **68** 1208
[10] Capeheart T W and Fisher M E 1976 *Phys. Rev.* B 13, 5021
[11] Lin D L, Che H and Xia Y 1992 *Phys. Rev.* A **46** 1805
[12] Lin D L, Che H, Lai W and George T F 1994 *Phys. Rev.* E **49** 2155
[13] Schulz B and Baberschke K 1996 Private communication. The Gd data are included just to show the general trend of thickness dependence.
[14] Ou J T, Wang F R and Lin D L 1997 *Phys. Rev.* E to be published
[15] Zheng X, Tan C-I and Chen T 1982 *Phys. Rev.* D **26** 1843
[16] Zheng X, Tan Z G and Wang J 1987 *Nucl. Phys.* B **287** 171
[17] Ou X F, Ou J T and Lin D L 1996 *Mod. Phys. Lett.* B **10** 531
[18] Griffiths R B 1972 *Phase Transitions and Critical Phenomena* vol 1, ed C Domb and M S Green (Academic) pp 72–7
[19] Rado G T 1957 *Bull. Am. Phys. Soc.* **112** 127
[20] Mills D L and Maraduddin A A 1967 *J. Phys. Chem. Solids* **28** 1855
[21] Mathon J 1988 *Physica* B **149** 31
[22] Tang H, Weller D, Walker T G, Scott J C, Chappert C, Hopster H, Pang A W, Dessau D S and Pappas D P 1993 *Phys. Rev. Lett.* **71** 444
[23] Liu G and Gradmann U 1993 *J. Magn. Magn. Mater.* **118** 99
[24] Ou J T and Lin D L 1994 *Chin. J. Phys.* **32** 703